Inorganic Chemistry

Article

pubs.acs.org/IC

Bisdithiazolyl Radical Spin Ladders

Kristina Lekin,[†] Joanne W. L. Wong,[†] Stephen M. Winter,[†] Aaron Mailman,[†] Paul A. Dube,[‡] and Richard T. Oakley*[,†]

[†]Department of Chemistry, University of Waterloo, Waterloo, Ontario N2L 3G1, Canada

[‡]Brockhouse Institute for Materials Research, McMaster University, Hamilton, Ontario L8S 4M1, Canada

Supporting Information

ABSTRACT: A series of four bisdithiazolyl radicals **1a**–**d** (R_1 = Pr, Bu, Pn, Hx; R_2 = F) has been prepared and characterized by X-ray crystallography. The crystal structure of **1a** (R_1 = Pr) belongs to the tetragonal space group $P\bar{4}2_1m$ and consists of slipped π-stack arrays of undimerized radicals packed about $\bar{4}$ centers running along the z-direction, an arrangement identical to that found for **1** (R_1 = Et; R_2 = F). With increasing chain length of the R_1 substituent, an isomorphous set **1b**–**d** is generated. All three compounds crystallize in the $P2_1/c$ space group and consist of pairs of radical π-stacks locked together by strong intermolecular F···S′ bridges to create spin ladder arrays. The slipped π-stack alignment of radicals produces close S···S′ interactions which serve as the "rungs" of a spin ladder, and the long chain alkyl substituents (R_1) serve as buffers which separate the ladders from each other laterally. Variable temperature magnetic susceptibility measurements indicate that **1a** behaves as an antiferromagnetically coupled Curie–Weiss paramagnet, the behavior of which may be modeled as a weakly coupled AFM chain. Stronger antiferromagnetic coupling is observed in **1b**–**d**, such that the Curie–Weiss fit is no longer applicable. Analysis of the full data range (T = 2–300 K) is consistent with the Johnston strong-leg spin ladder model. The origin of the magnetic behavior across the series has been explored with broken-symmetry Density Functional Theory (DFT) calculations of individual pairwise exchange energies. These confirm that strong antiferromagnetic interactions are present *within* the ladder "legs" and "rungs", with only very weak magnetic exchange *between* the ladders.

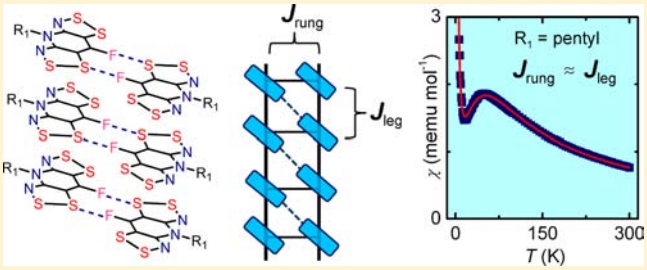

INTRODUCTION

The pursuit of neutral radicals as nonmetal based single-component molecular materials capable of serving as carriers of spin and charge has a long history. Almost 40 years ago Haddon proposed that in the solid state, arrays of organic π-radicals, each contributing one electron to a half-filled ($f = {}^1/_2$) energy band, should be capable of exhibiting metallic conductivity.[1] Experimentally, this goal has not been easy to achieve, although much progress has been made with the use of odd-alternant hydrocarbons, that is, phenalenyls and spiro-phenalenyls.[2,3] Light heteroatom (N, O) radicals such as nitroxyls,[4] verdazyls,[5] and triazinyls[6] have also been pursued, as the presence of the heteroatom(s) helps suppress dimerization. At the same time, however, the localization of spin density on light heteroatoms reduces intermolecular overlap and compromises conductivity. Nonetheless, while localized spins are not beneficial for conductivity, they facilitate the design of magnetic materials. Consistently, light heteroatom radicals were the first to exhibit both ferromagnetic[7] and canted antiferromagnetic[8] ordering.

The incorporation of heavier heteroatoms such as sulfur and selenium into organic frameworks offers, in principle, the benefit of improved intermolecular overlap and hence enhanced charge transport properties. For many years, work on this idea focused on monocyclic radicals based on dithiadiazolyl and dithiazolyl building blocks.[9] Generally, however, charge transport in these early systems was compromised by dimerization,[10] although when this was avoided some remarkable magnetic effects were observed.[11] Eventually, expansion of the framework to include resonance delocalization, as in the bisdithiazolyl frameworks **1** and **2** (Chart 1),[12,13] led to undimerized $S = {}^1/_2$ systems exhibiting higher conductivity, with σ(300 K) reaching 2×10^{-2} S cm^{-1} for **3** (R = F).[12d]

In addition to facilitating the development of conductive materials, bisdithiazolyl radicals have proven of value for their magnetic properties. For example, canted antiferromagnetic (AFM) ordering has been observed in **3** (R = Ph, Cl, F),[13] and

Chart 1

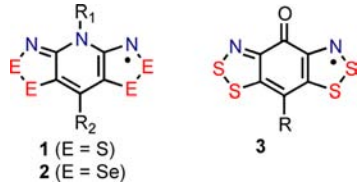

Received: December 4, 2012
Published: February 7, 2013

   dx.doi.org/10.1021/ic302658c | *Inorg. Chem.* 2013, 52, 2188–2198

field induced ferromagnetic (FM) ordering in **1** (R_1 = Me, R_2 = H)[14] and **3** (R = Ph).[13] The involvement of spin−orbit coupling[15] occasioned by the incorporation of selenium into the ring system of **2** has also led to Dzyaloshinsky−Moriya spin-canted AFM ordering with T_N = 28 K for R_1 = Et, R_2 = H.[16] Ferromagnetic ordering with T_C values as high as 17.5 K and coercive fields H_c of 1600 Oe (at 2 K) for R_1 = Et, R_2 = Br has also been observed.[17] At the same time, selenazyl radicals **2** enjoy improved charge transport properties relative to their sulfur counterparts **1**.[18]

One of the main advantages of materials research based on the use of molecular building blocks is the ability to fine-tune physical properties at the chemical level. In this regard the solid state crystal structures of radicals **1**−**3** are highly sensitive to the nature of ligands R_1 and R_2, with dramatic changes in space group and solid state architecture arising from seemingly minor modifications. In recent work on derivatives of **3** we have shown that the incorporation of structure-making intermolecular contacts (supramolecular synthons)[19] can afford a degree of structural control.[13] In particular we have observed that a fluorine atom in the basal R position of **3** plays a major role by means of strong intermolecular F···S′ interactions.[13d]

In the present work we extend our exploration of the packing patterns and physical behavior of **1** as a function of R_1/R_2. Our strategy has been based on the idea of fixing R_2 = F, with the intention of generating specific packing motifs by means of intermolecular F···S′ contacts. Given the anticipated "pinning effect" of such interactions, we hoped to monitor the variation of structure and property with a steady increase in the size of the R_1 group. To this end we have synthesized four new bisdithiazolyl radicals **1a**−**d** (Chart 2, R_1 = Pr, Bu, Pn, Hx),

Chart 2

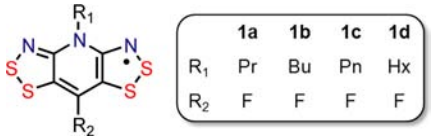

	1a	1b	1c	1d
R_1	Pr	Bu	Pn	Hx
R_2	F	F	F	F

three of which have alkyl chains longer than any bisdithiazolyl reported to date. While the propyl derivative **1a** crystallizes in the familiar tetragonal space group $P\bar{4}2_1m$, like the corresponding compound where R_1 = Et,[20] the remaining three have a common but hitherto unobserved packing pattern. This finding is particularly interesting from the perspective of crystal engineering, as the structures of **1b**−**d** are all based on the anticipated pairs of radicals "pinned" together by strong S···F′ interactions (Figure 1A). This feature, coupled with the long alkyl chains on either end leads, almost inexorably, to π-stacking of pairs of radicals in a ladder-like geometry displaying classic spin ladder magnetic behavior.

The observation of spin coupling along one-dimensional (1D) arrays of magnetically active centers, to afford FM or AFM coupled chains, is common. Lateral coupling of two magnetic chains can lead to a spin-ladder (Figure 1B), where interactions between (J_{rung}) and within (J_{leg}) the magnetic chains may be FM or AFM; the ideal spin-ladder being such that $J_{rung} = J_{leg}$.[21] To date the most thoroughly studied ladders are built from transition metal complexes of copper,[22,23] but molecular radical[24] and radical ion[25] ladders, which are easier to study because of the presence of weaker interactions, have also been reported. In all cases the interest in these systems lies in

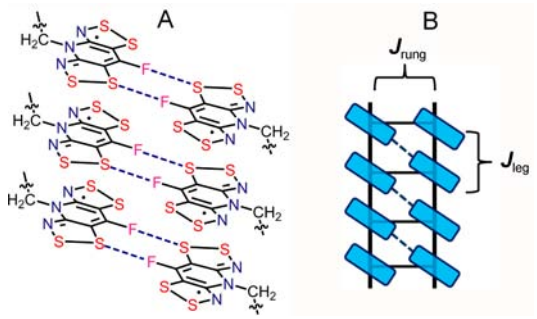

Figure 1. Intermolecular S···F′ contacts (supramolecular synthons) that lock radicals laterally into centrosymmetic pairs (A), and ladderlike arrays produced by π-stacking of these pairs (B).

the existence of an energy gap in the spin excitation spectrum,[26] which has possible relationships to high-temperature superconductivity for lightly doped even-legged ladders.[27] The presence of ladder-like π-stacking in **1b**−**d** has prompted a thorough analysis of their magnetic properties as a function of temperature. The results have been interpreted in the light of broken symmetry Density Functional Theory (DFT) calculations and magnetic simulations based on various spin ladder models.

RESULTS AND DISCUSSION

Synthesis and EPR Spectra. The preparation of **1a**−**d** began with the alkylation of 2,4,6-trifluoropyridine **4** with the appropriate alkyl trifluoromethanesulfonate (triflate)[28] to generate the alkylated pyridinium triflate **5** as an ionic liquid at room temperature. Ammonia gas was then gently bubbled into a solution of **5** in MeCN to afford the *N*-alkyl-2,6-diamino-4-fluoropyridinium triflate salt **6**, which was crystallized as white needles from water (Scheme 1). The latter compound

Scheme 1

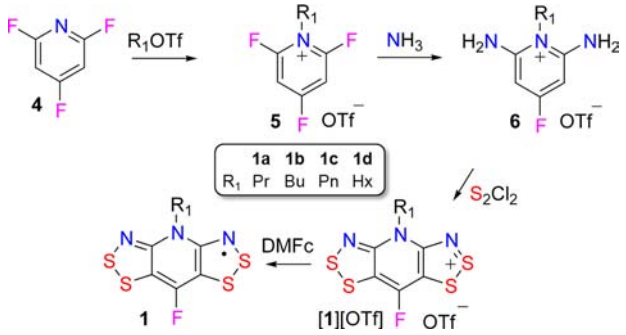

undergoes a double Herz cyclization reaction with S_2Cl_2 in refluxing MeCN to give bright red shard-like crystals of the bisdithiazolylium triflate salt [**1**][OTf]. Reduction of this salt with decamethylferrocene (DMFc) in degassed MeCN generated the desired radicals **1a**−**d** in good yield. Single crystals suitable for X-ray analysis of **1a,b** were grown via vacuum sublimation, while long needles of **1c,d** were generated by recrystallization from carefully degassed (four freeze−pump−thaw cycles) heptane.[29]

While radicals **1** (R_1 = Me, Et, Pr; R_2 = Cl) were fully characterized in previous work,[12] no attempts were made at the time to extend the length of the alkyl chain R_1 beyond a propyl derivative. To compare the transport properties of **1b**−**d** to the

dx.doi.org/10.1021/ic302658c | Inorg. Chem. 2013, 52, 2188−2198

related compounds **1** (R_1 = Bu, Pn; R_2 = Cl), with long alkyl chain R_1 groups but with a chlorine (rather than a fluorine) atom in the R_2-position, the appropriate bisdithiazolylium triflate salts [**1**][OTf] were synthesized. However, while the chloro-substituted radicals could be successfully generated via reduction with DMFc, attempts to recrystallize them using similar methods to those used for the fluoro-substituted radicals led to poorly formed microcrystalline material. These results emphasize the apparent importance of the fluorine substituent as a structure-maker; an issue that will be explored more fully below.

Electron paramagnetic resonance (EPR) studies on **1a–d** provided confirmation of a highly delocalized spin distribution as observed in related compounds. The X-band EPR spectrum (recorded at ambient temperature in dichloromethane) shown in Figure 2 displays the characteristic[12] five-line hyperfine

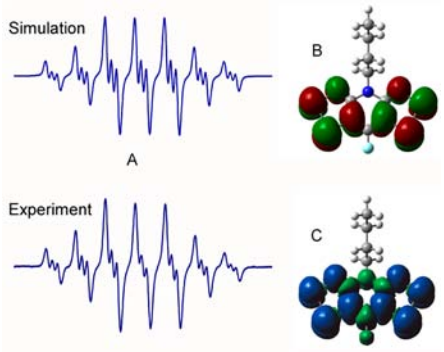

Figure 2. (A) Experimental (bottom) and simulated (top) EPR spectrum of **1b** in CH_2Cl_2, SW = 4 mT, LW = 0.030 mT. (B) B3LYP/6-31G(d,p) SOMO and (C) spin density distribution for **1b**.

pattern from spin coupling to two equivalent ^{14}N (I = 1) nuclei on the dithiazolyl rings superimposed on the two-line pattern arising from the large coupling to the basal ^{19}F (I = $^1/_2$) nucleus. As expected, the hyperfine coupling constants are very similar across the series of radicals. There is additional fine structure present from weaker coupling to the central nitrogen atom, with no variation across the series **1a–d**. Details from the simulation are provided in Table 1.

Table 1. EPR[a] Parameters for Radicals 1a–d

	1a	1b	1c	1d
a_N (S), mT	0.317	0.318	0.311	0.318
a_N (R_1), mT	0.056	0.056	0.056	0.056
a_H (CH_2), mT	0.020	0.020	0.016	0.021
a_F, mT	0.623	0.622	0.637	0.621
L/G	0.25	0.15	0.15	0.15
LW (mT)	0.030	0.030	0.040	0.030
g-value	2.00879	2.00871	2.00875	2.00880

[a]Derived hyperfine coupling constants and g-values extracted by simulation with Simfonia.[30]

Crystallography. The crystal structures of **1a–d** have been determined at ambient temperature by single-crystal X-ray diffraction. Crystal metrics for the four structures are provided in Table 2, and ORTEP drawings (50% probability ellipsoids) of the molecular units, showing atom numbering schemes, are illustrated in Figure 3. Pertinent intermolecular distances are provided in Table 3.

The tetragonal unit cell motif found for **1a** is not new, and has been observed in the past in many bisdithiazolyls and their selenium variants. In particular, the structure of **1a** is reminiscent of the kinetically favored α-phase of **1** (R_1 = Et, R_2 = F)[20] and also that found for **1** (R_1 = Et, Pr; R_2 = Cl).[17b] The radicals (Figure 3A) are bisected by mirror planes perpendicular to the xy-plane, and pack in 4-fold pinwheel-like clusters around the $\bar{4}$-point (Figure 4). They form slipped π-stack arrays running along the z-direction, and the mean interplanar separation (δ) of 3.479 Å between radical plates is similar to that of related bisdithiazolyls **1** (R_1 = Et, R_2 = F, Cl). More details of the structure of **1a**, including a side view of the π-stacks and a list of intermolecular contacts, are provided in the Supporting Information.

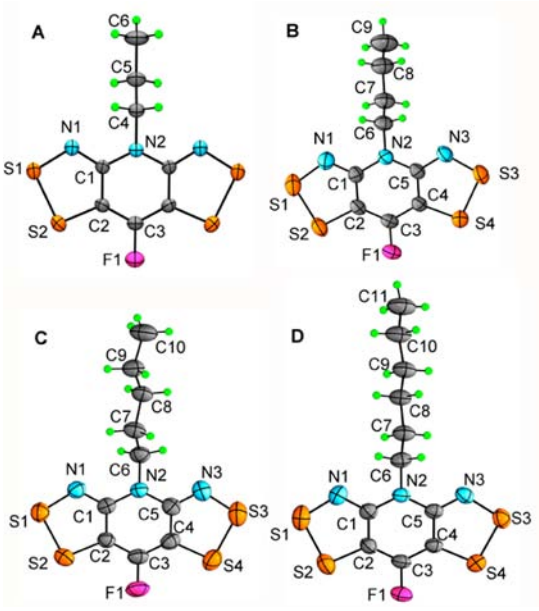

Figure 3. ORTEP drawings (50% probability ellipsoids) of the four molecules **1a–d** (A–D, respectively) showing the atom numbering scheme.

All the longer chain alkyl-substituted radicals **1b–d** crystallize as an isomorphous set within the monoclinic space group $P2_1/c$. It is apparent, then, that the variations in crystal packing attributed to modifications in R_1 cease once the length of the alkyl chain is sufficiently large. Beyond this point the packing is controlled by the combined effects of (i) the nonpolar organic groups, which tend to keep the radicals apart, and (ii) strong intermolecular F···S′ interactions, which cause the radicals to link laterally in a pairwise fashion (Figure 1). The net result is that radicals form slipped, cross-braced π-stack arrays running along the y-direction, as may be seen in Figure 5, which shows a projection of the crystal packing along the z-direction.

The spin ladders in **1b–d** are based on building blocks of pairs of radicals pinned together by two F···S′ (d_2) bridges, and locked into slipped π-stacks by S···S′ (d_1) with π–π interactions which form the ladder "rungs" and "legs", respectively (Figure 6). The F···S′ distances (Table 3) are well within the sum of the van der Waals separation for F and S (3.27 Å),[31] and the shortness and hence strength of these contacts may well contribute significantly to the stability of the crystal structures, a hypothesis supported by the difficulties encountered in growing

dx.doi.org/10.1021/ic302658c | Inorg. Chem. 2013, 52, 2188–2198

Table 2. Crystal Data

	1a	1b	1c	1d
formula	$C_8H_7FN_3S_4$	$C_9H_9FN_3S_4$	$C_{10}H_{11}FN_3S_4$	$C_{11}H_{13}FN_3S_4$
M	292.42	306.43	320.50	334.52
a, Å	15.9560(7)	15.6371(12)	17.8728(10)	18.0351(17)
b, Å	15.9560(7)	4.8733(4)	4.6091(3)	4.6620(4)
c, Å	4.2769(2)	17.0938(13)	17.0345(9)	17.1669(16)
β, deg	90	108.6200(10)	108.466(2)	98.334(2)
V, Å	1088.87(8)	1234.44(17)	1331.01(13)	1428.1(2)
ρ_{calcd} (g cm^{-1})	1.784	1.649	1.599	1.556
space group	$P\bar{4}2_1m$	$P2_1/c$	$P2_1/c$	$P2_1/c$
Z	4	4	4	4
temp (K)	296(2)	296(2)	295(2)	296(2)
μ (mm^{-1})	0.858	0.761	6.552	0.665
λ (Å)	0.71073	0.71073	1.54178	0.71073
data/restr./parameters	1649/0/83	2983/0/155	2324/0/163	2647/0/172
solution method	direct methods	direct methods	direct methods	direct methods
R, R_w (on F^2)	0.0214, 0.0564	0.0394, 0.0675	0.0456, 0.1134	0.0413, 0.0828

Table 3. Intermolecular Structural Parameters (in Å)

		1b	1c	1d
d_1	S4···S2′	3.689	3.797	3.742
d_2	F1···S2′	3.210	3.198	3.232
d_3	S1···S2′	3.593	3.946	3.763
d_4	S1···S2′	3.453	3.447	3.411
d_5	S1···S1′	3.618	3.586	3.580
d_6	S2···N3′	3.089	3.288	3.187
δ		3.42	3.56	3.54
dx		1.86	2.32	2.08
dy		2.93	1.78	2.21

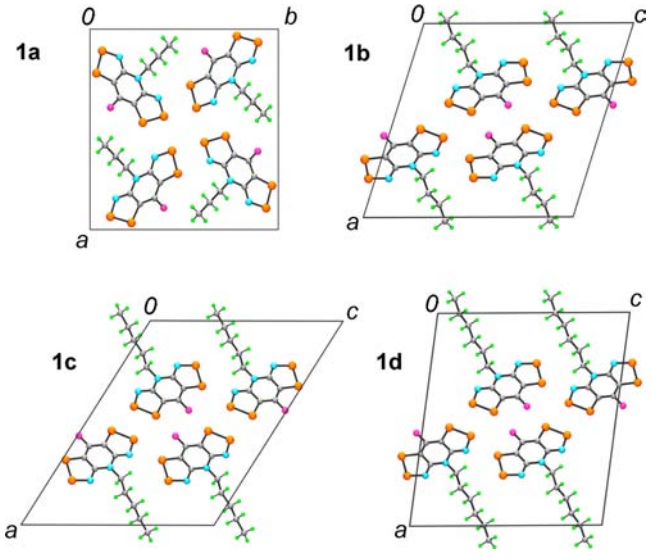

Figure 4. Unit cell projections parallel to the stacking axes for **1a–d**.

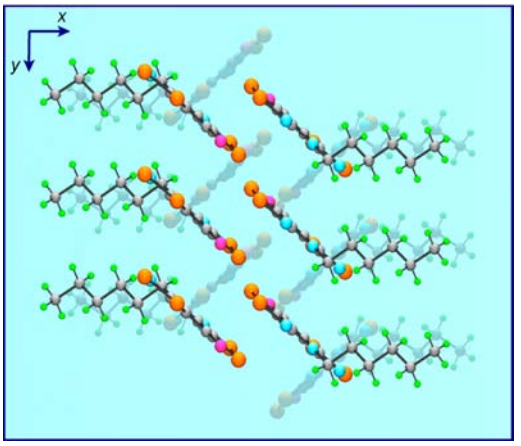

Figure 5. π-Stacking in **1d**, viewed down the z-axis, illustrating cross-braced nature of adjacent spin ladders.

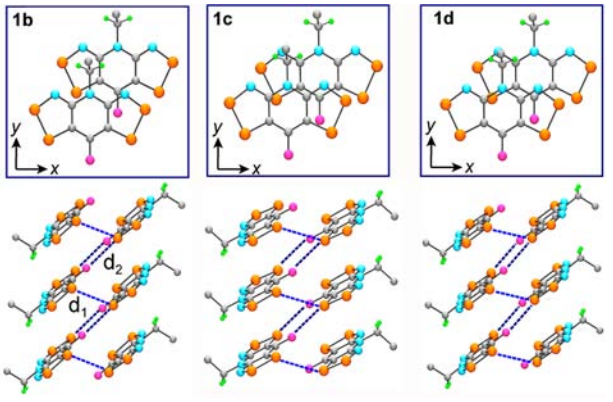

Figure 6. Views along the top illustrate the slippage of adjacent radicals in **1b–d** along the π-stacks in local coordinates x and y. The views along the bottom demonstrate the ladder-like packing and contacts d_1 (S4···S2′) and d_2 (F1···S2′). For clarity, the alkyl chains have been truncated after C2.

crystals of the corresponding chloro-substituted radicals **1** (R_1 = Bu, Pn; R_2 = Cl). Planar supramolecular assemblies stemming from the F···S′ synthons have been observed before in thiazyl radical structures.[13d]

Adjacent ladders along the z-direction are connected by a series of weak S···S′ and S···N′ contacts (d_3-d_6), as shown in Figure 7. Interactions of similar magnitude have been observed in other bisdithiazolyl structures, and their magnetic implications are discussed below. The bulkiness of the alkyl chains drives the radical plates to tilt and slip severely in both the lateral (local y coordinate) and longitudinal (local x coordinate) directions. As may be seen in Figure 6 and Table 3, the extent and direction of stack slippage varies across the series. Slippage along x (dx) is greatest for **1c** while movement

dx.doi.org/10.1021/ic302658c | Inorg. Chem. 2013, 52, 2188–2198

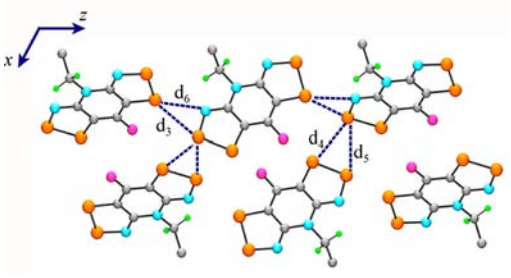

Figure 7. View down the π-stacking axis (y-direction) for **1b–d** showing interladder contacts d_3-d_6. For clarity, the alkyl chains have been truncated after C2.

along y (dy) is the smallest (Table 3). As a result, the intermolecular S···S′ distances d_3 (3.946 Å) and d_6 (3.288 Å) found for **1c** are significantly larger than the respective lengths for **1b**,**d**, where d_3 and d_6 range 3.593–3.763 and 3.089–3.187 Å, respectively. Lateral extension of ladders along the z-direction, linked by these weak contacts generates a pseudo 2D trellis in the yz plane, with long chain alkyl groups protruding from either side. Packing of the layers then affords a wafer-like assembly (Figure 8), with interdigitized alkyl groups creating a hydrocarbon buffer, separating neighboring layers from one another.

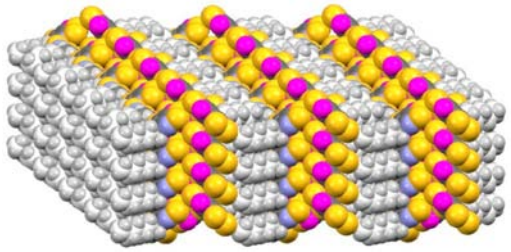

Figure 8. Space-filling diagram displaying wafer-like packing of **1d**. The long alkyl chains along the yz-plane separate the spin centers.

Magnetic Measurements. Variable temperature magnetic susceptibility (χ) measurements have been performed on **1a–d** over the temperature range 2–300 K using a SQUID magnetometer operating at a field (H) of 1000 Oe. Figure 9 shows the results for **1a** presented in the form of plots of χ (corrected for diamagnetic contributions) versus T and χT against T (inset).

The tetragonal phase **1a** behaves as a Curie–Weiss paramagnet, and a fit to the 20–300 K data affords values of

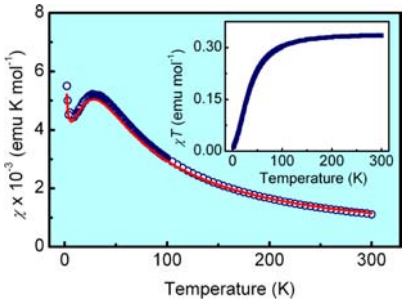

Figure 9. Field-cooled χ and χT (inset) versus T plots for **1a** at H = 1000 Oe. Solid red line indicates calculated χ from Bonner–Fisher AFM $S = {}^1/_2$ chain magnetic model.[32].

C = 0.355 emu K mol^{-1} and θ = −16.5 K. The data were also modeled in terms of a Heisenberg chain of AFM coupled $S = {}^1/_2$ radicals, using a fit function based on the molecular-field modified Bonner–Fisher method[32] and the Heisenberg Hamiltonian $H_{ex} = -2J\{S_1 \cdot S_2\}$.[33] The intrachain AFM exchange energy of J = −15.5 cm^{-1} extracted from the 1D chain model is comparable to the value of J = −9.6 cm^{-1} obtained for the related compound **1** (R_1 = Et, R_2 = F, α-phase). The somewhat stronger AFM coupling found for **1a** may be attributed to an increase in the π-stack slippage (along only the y-direction) associated with a longer alkyl substituent on the tetragonal bisdithiazolyl ring system.[17b,34]

By contrast, χT versus T plots for radicals **1b–d** demonstrate significantly stronger antiferromagnetic (AFM) coupling than that found for **1a**. Attempts to fit the data to a Curie–Weiss paramagnet model were unsuccessful, providing unreasonably large θ values. Other models which we explored were the Bonner–Fisher 1D AFM chain, as well as the Bleaney–Bowers dimer,[35] neither of which provided a satisfactory fit. However, an understanding of the crystal structures led us to the spin ladder model outlined by Gu, Yu, and Shen[36] and popularized by Landee,[37] with which we did have marginal success for an incomplete data range (50–300 K) (See Supporting Information for details). The unsatisfactory fit was attributed to the limitations of this model, which assumes that interactions within the ladder "rungs" (J_{rung}) are much stronger than those along the "legs" (J_{leg}). This condition is not satisfied in the present systems.

On the other hand, the ladder models developed by Johnston et al. from fits to quantum Monte Carlo (QMC) simulations of $J_{leg} \approx J_{rung}$ ladders provided a much more satisfying fit over the entire temperature range.[38] The results, which are tabulated in Table 4 and displayed graphically in Figure 10 (red line),

Table 4. Magnetic Modeling Results

	1a	1b	1c	1d
J_{leg} (cm^{-1})	−16[a]	−66	−26	−57
J_{rung} (cm^{-1})	−1.3[b]	−17	−26	−13
PM impurity (%)	13.4	2.8	4.2	6.1
Δ (cm^{-1})	0[c]	8.0	13.1	5.3

[a]Fit with Bonner–Fisher AFM chain. Term J_{leg} applies to intrachain interaction. [b]Term J_{rung} applies to zJ' term. [c]Compound **1a** is an AFM chain, as a result Δ = 0.

indicate that all three compounds **1b–d** behave as two-legged spin ladders. The radicals with even-numbered alkyl chains **1b** and **1d** have comparable J values; both demonstrate strong leg interactions and much weaker rung interactions. By contrast, the pentyl substituted radical **1c** is an ideal spin ladder by virtue of its strong, yet approximately equal J_{leg} and J_{rung} interactions (−26 cm^{-1}). Correspondingly, the spin gap (Δ) for **1c** is greater than that for the remaining three radicals because it is the least chain-like.

While it is possible to include terms for interladder magnetic interactions, the buffering effect of the long alkyl chains in radicals **1b–d** isolates the ladders in at least the x-direction. There are, however, numerous close contacts (d_3-d_6) between neighboring ladders along the z-direction that may give rise to significant magnetic exchange. In an attempt (i) to explore the validity of the isolated ladder model for **1b–d** and (ii) to understand more clearly the magnetic exchange pathway within these ladders, we performed a series of pairwise broken-

dx.doi.org/10.1021/ic302658c | Inorg. Chem. 2013, 52, 2188–2198

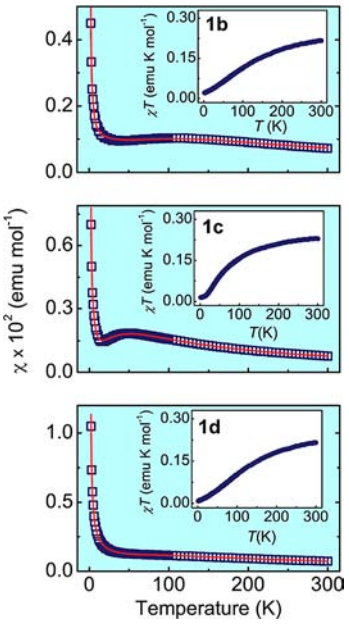

Figure 10. Field-cooled χ and χT (insets) versus T plots for **1b–d** (respectively) at H = 1000 Oe. Solid red lines indicate calculated χ from strong-leg spin ladder model by Johnston et al.[38].

symmetry DFT calculations.[39,40] In addition to the exchange energy associated with neighboring radicals within the π-stack J_π, there are four symmetry independent pathways corresponding to J_1–J_4, all illustrated in Figure 11.

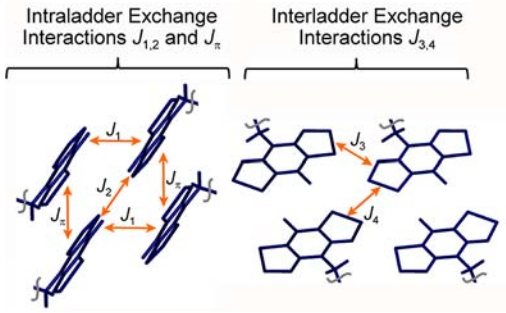

Figure 11. Pairwise exchange interactions J_1, J_2, J_3, J_4, and J_π.

The numerical results from these single-point calculations (Table 5) prompt several observations. First, J_π and J_1 (associated with the "legs" and "rungs" of the ladder, respectively) are strongly AFM, supporting the notion that the assembled radicals form a completely AFM coupled spin ladder. Second, the J_π for **1c** is significantly smaller in magnitude than the other two (**1b**,**d**), which is consistent with the results obtained from the Johnston strong-leg ladder fit. The drastically different slippage of this radical, as shown in Figure 6 (top), with an odd-chain length hydrocarbon (pentyl) substituent likely gives rise to dramatically different overlap of the singly occupied molecular orbitals (SOMOs) along the π-stacks. As a result, the magnetic exchange in this direction, and the apparently anomalous magnetic response of **1c**, is not unexpected.

Table 5. UB3LYP/6-31G(d,p) Exchange Energies[a]

	1b	1c	1d
J_π	−33.73	−9.10	−31.35
J_1	−50.37	−46.46	−65.89
J_2	0.44	0.08	0.19
J_3	3.09	0.83	1.41
J_4	3.01	−1.45	2.06

[a]In cm^{-1}, from single-point calculations (See Supporting Information).

Finally, the small values associated with magnetic exchange parameters J_2–J_4 auger well for the independence of the individual ladders. Although, crystallographically there are interactions between ladders running along the z-direction because of the close proximity of the radical plates, these contacts do not lead to strong magnetic exchange. However, in all cases across the series, the value for the magnetic exchange parameter J_1 (rung) is greater than J_π (leg), which is opposite of the result of the magnetic modeling.

To explore the magnetic properties suggested by the calculated exchange parameters, we simulated the magnetic susceptibility by using both exact diagonalization (ED) methods on small clusters of up to 12 radicals, and QMC simulations on extended ladders.[41,42] In each case the DFT computed exchange energies provided in Table 5 were employed. Unfortunately, not all interactions J_π, J_{1-4} could be included in the QMC simulations because the nonbipartite nature of the full magnetic lattice leads to a sign problem. However, as might be expected, the ED calculations suggest that the interactions *between* ladders (J_{2-4}) are small, and their inclusion does not lead to significant difference in the simulated susceptibility. As a result the systems were treated as approximately *isolated* spin ladders, that is, the QMC simulations were carried out including only J_π (leg) and J_1 (rung) interactions. The model systems were chosen to be large enough that finite size effects were negligible.

The QMC results are shown graphically in Figure 12, compared with the observed response once the paramagnetic

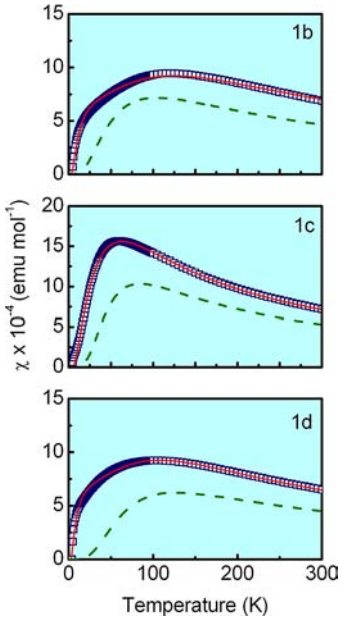

Figure 12. Quantum Monte Carlo (QMC) simulations on extended ladders of **1b–d** (green dashed line), along with the experimental SQUID data (blue squares) and Johnston strong-leg ladder[38] fit (red line) with the subtraction of the paramagnetic impurity.

dx.doi.org/10.1021/ic302658c | Inorg. Chem. 2013, 52, 2188–2198

impurity suggested by fitting is subtracted. In all cases, the simulated susceptibility converges to zero at low temperatures more rapidly than was observed. This can be rationalized by considering the large and small J_{leg}/J_{rung} limits: when $J_{leg} \gg J_{rung}$, the system should behave as isolated $S = {}^1/_2$ AFM chains with no spin gap, whereas when $J_{leg} \ll J_{rung}$, the system should behave as isolated AFM coupled dimers, with an exponentially decaying susceptibility at low temperatures because of a sizable spin gap. The discrepancy between the observed and the simulated data can therefore be traced to the difference in computed and fit exchange parameters; fitting suggests stronger leg interactions, while the DFT calculations suggest stronger rung interactions. We therefore conclude that the so-called *bottom-up* methodology[40a] provides the correct qualitative picture of isolated spin-ladders. However, the quantitative details, such as the ratio J_{leg}/J_{rung}, do not match the fitting results or experiment.

SUMMARY AND CONCLUSIONS

With elongation of the alkyl R_1 substituent beyond three carbons, the crystal packing of π-stacked bisdithiazolyl radicals **1** bearing basal fluorine substituents (R_2 = F) changes abruptly. Thus, when R_1 = Et, Pr, the radical π-stacks are locked into pinwheel clusters, but with R_1 = Bu, Pn, Hx, adjacent columns of π-stacked radicals are bridged by short intermolecular F···S′ contacts to produce $S = {}^1/_2$ spin ladder arrays. While the discovery of the role of F···S′ interactions in influencing crystal packing in the present family of radicals is somewhat opportune, the notion that fluorine can, by virtue of its high electronegativity, play an important role as a supramolecular structure-maker is by no means new. For example, we have recently observed that intermolecular H_3C···F′ interactions can facilitate the interlocking of neighboring radical π-stacks.[43] It is also well-established in nitroxyl radical structures that covalently bound fluorine atoms have the potential to enter into weak "hydrogen bridge" interactions.[44] It is thus not surprising that the electronegative fluorine atom in structures **1b−d** is strongly attracted to the neighboring electropositive sulfur. The resulting centrosymmetric linking of radicals places the long alkyl chains in opposite directions, in prime position for interdigitization and the assembly of a molecular ladder.

As expected from its appearance, the magnetic properties of **1b−d** are consistent with spin ladder behavior. DFT broken symmetry calculations suggest that slippage of the π-stacks affords strong AFM exchange along the legs of the ladder, while the lateral S···S′ overlap gives rise to strong AFM exchange across its rungs. Consistently the experimental magnetic data for all three radicals can be fit to a strong leg spin ladder model. This procedure also reveals that in **1b,d** AFM exchange interactions along the ladder legs are significantly stronger than those along the rungs. By contrast, **1c** displays ideal spin ladder behavior, with interactions along the legs and rungs being approximately equal. In a broader context, the present results provide a further demonstration of the diversity in structure and property that can be achieved by judicious modification of the R_1/R_2 substituents of bisdithiazolyls. Rich opportunities for the design of property-specific materials lie ahead for these and other related radicals.

EXPERIMENTAL SECTION

General Procedures and Starting Materials. The reagents hexamethyldisilazane, *N*-bromo-succinimide, trifluoromethanesulfonic anhydride, 2,4,6-trifluoropyridine, sulfur monochloride, and decamethylferrocene (DMFc) were obtained commercially from Aldrich and SynQuest, unless otherwise stated. All were used as received save for DMFc, which was sublimed in vacuo and recrystallized from acetonitrile before use. The alkylated triflates were prepared according to literature methods.[16] The solvents acetonitrile (MeCN), dichloroethane (DCE), and dichloromethane (DCM) were of at least reagent grade. MeCN was dried by distillation from P_2O_5 and/or CaH_2, and both DCE and DCM by distillation from P_2O_5. All reactions were performed under an atmosphere of dry nitrogen. Melting points are uncorrected. Fractional sublimations were performed in an ATS series 3210 three-zone tube furnace, mounted horizontally, and linked to a series 1400 temperature control system. Infrared spectra (Nujol mulls, KBr optics) were recorded on a Nicolet Avatar FTIR spectrometer at 2 cm^{-1} resolution. ^1H NMR spectra were run on a Bruker Avance 300 MHz NMR spectrometer and low resolution Electro-Spray Ionization (ESI) mass spectra were run on a Micromass Q-TOF Ultima Global LC/MS/MS system. Elemental analyses were performed by MHW Laboratories, Phoenix, AZ 85018.

Preparation of *N*-propyl-2,4,6-trifluoro-pyridinium Trifluoromethanesulfonate 5 (R_1 = Pr). In a Schlenk tube under N_2, propyl triflate (3.0 g, 15.6 mmol) was added to 2,4,6-trifluoropyridine **4** (1.73 g, 13.0 mmol), and the mixture was stirred and heated at 60 °C overnight. The colorless oil was analyzed by ^1H NMR in CD_3CN and compared to other known compounds.[20,45] After removing volatiles in vacuo, the material was carried forward without further purification.

Preparation of *N*-propyl-2,6-diamino-4-fluoropyridinium Trifluoromethanesulfonate 6 (R_1 = Pr). The product **5** (R_1 = Pr, ∼ 4.2 g, ∼ 13 mmol) was dissolved in 50 mL of MeCN and cooled in an ice bath, over which ammonia gas was passed for 15 min, generating NH_4F as a white precipitate. The NH_4F was filtered off, and the solvent flash evaporated to leave a white crystalline powder, which was recrystallized from 18 mL of H_2O to afford colorless crystals of **6** (R_1 = Pr), yield: 2.20 g (6.90 mmol, 53% over two steps); mp 179−181 °C. IR: 3426 (s), 3362 (s), 3247 (s), 3108 (m), 1671 (s), 1651 (s), 1634 (s), 1612 (s), 1513 (s), 1489 (m), 1340 (m), 1259 (s), 1227 (s), 1173 (s), 1082 (m), 1082 (w), 1032 (s), 1016 (m), 808 (m), 638 (s), 598 (w), 582 (w), 572 (w), 524 (m), 515 (m) cm^{-1}. Anal. Calcd for $C_9H_{13}F_4N_3O_3S$: C, 33.86; H, 4.10; N, 13.16. Found: C, 34.04; H, 4.30; N, 12.96.

Preparation of 8-Fluoro-4-propyl-4*H*-bis([1,2,3]dithiazolo)-[4,5-*b*:5′,4′-*e*]pyridin-2-ium Trifluoromethanesulfonate [1a][OTf]. The *N*-propyl pyridinium triflate salt **6** (4.02 g, 12.6 mmol) was dissolved in 24 mL of a 3:1 v/v mixture of DCE and MeCN under nitrogen. S_2Cl_2 (4.04 mL, 50.4 mmol) was added via syringe, and the solution was refluxed for 2.5 h. After the allotted reaction time, the dark green solution was cooled to ambient temperature and then to 0 °C. The red crystals were isolated by filtration, then washed with 3 × 10 mL of DCE to give a crude yield of 4.93 g. The product [**1a**][OTf] was dissolved in 100 mL of hot HOAc, the solution hot filtered and concentrated to 60 mL, then cooled to room temperature. The red lustrous crystals were filtered off and washed with DCE, yield 3.50 g (7.94 mmol, 63%); mp 259−260 °C. IR: 1507 (s), 1369 (s), 1353 (m), 1268 (s), 1243 (s), 1226 (m), 1181 (w), 1171 (w), 1117 (w), 1102 (w), 1087 (w), 1027 (s), 789 (s), 714 (w), 680 (m), 670 (w), 650 (w), 638 (s), 473 (s) cm^{-1}. Anal. Calcd for $C_9H_7F_4N_3O_3S_5$: C, 24.48; H, 1.60; N, 9.52. Found: C, 24.74; H, 1.90; N, 8.85.

Preparation of 8-Fluoro-4-propyl-4*H*-bis([1,2,3]dithiazolo)-[4,5-*b*:5′,4′-*e*]pyridin-2-yl 1a. Decamethylferrocene (0.466 g, 1.43 mmol) was added to a solution of [**1a**] [OTf] (0.600 g, 1.36 mmol) in 14 mL of bubble degassed MeCN. The slurry was stirred at room temperature for 2 h. After the allotted reaction time, the brown, matte solid was filtered, washed with freshly distilled MeCN to give a green microcrystalline solid **1a** (0.365 g, 92%). Crystals suitable for crystallographic work, as well as transport property measurements, were obtained by vacuum sublimation of the bulk material at 10^{-4} Torr in a three-zone furnace along a temperature gradient of 140 to 60 °C; dec (in air) > 110 °C. IR: 1503 (m), 1432 (m), 1365 (m), 1315 (m), 1281 (m), 1226 (s), 1132 (w), 1097 (s), 1084 (m), 932 (w), 900 (w), 824 (s), 769 (s), 751 (s), 722 (w), 685 (s), 659 (s), 652 (s), 535

dx.doi.org/10.1021/ic302658c | *Inorg. Chem.* 2013, 52, 2188−2198

(m), 469 (s), 452 (m) cm^{-1}. Anal. Calcd for $C_8H_7FN_3S_4$: C, 32.86; H, 2.41; N, 14.37. Found: C, 33.02; H, 2.60; N, 14.06.

Preparation of *N*-butyl-2,4,6-trifluoro-pyridinium Trifluoromethanesulfonate 5 (R_1 = Bu). In a Schlenk tube under N_2, butyl triflate (3.0 g, 14.6 mmol) was added to 2,4,6-trifluoropyridine **4** (1.73 g, 13.0 mmol), and the mixture was stirred and heated at 60 °C overnight. The colorless oil was analyzed by ^{1}H NMR in CD_3CN and compared to other known compounds.[20,45] After removal of volatiles in vacuo, the material was carried forward without further purification.

Preparation of *N*-butyl-2,6-diamino-4-fluoropyridinium Trifluoromethanesulfonate 6 (R_1 = Bu). The product **5** (R_1 = Bu, ~ 4.4 g, ~ 13 mmol) was dissolved in 30 mL of MeCN and cooled in an ice bath, over which ammonia gas was passed for 15 min, generating NH_4F as a white precipitate. The NH_4F was filtered off, and the solvent flash evaporated to leave a white crystalline powder, which was recrystallized from 25 mL of DCE and MeCN (10:1) to afford colorless crystals of **6** (R_1 = Bu), yield: 2.76 g (8.28 mmol, 64% over two steps); mp 167−169 °C. IR: 3432 (s), 3362 (s), 3245 (s), 3107 (m), 2853 (s), 1668 (s), 1614 (s), 1548 (w), 1512 (s), 1489 (m), 1355 (m), 1336 (m), 1260 (s), 1226 (s), 1173 (s), 1119 (w), 1081 (m), 1032 (s), 1014 (s), 815 (s), 762 (m), 638 (s), 601 (w), 581 (w), 571 (w), 514 (m) cm^{-1}. Anal. Calcd for $C_{10}H_{15}F_4N_3O_3S$: C, 36.04; H, 4.54; N, 12.61. Found: C, 36.24; H, 4.40; N, 12.76.

Preparation of 8-Fluoro-4-butyl-4*H*-bis([1,2,3]dithiazolo)-[4,5-*b*:5′,4′-*e*]pyridin-2-ium Trifluoromethanesulfonate [1b][OTf]. The *N*-butyl pyridinium triflate salt **6** (3.0 g, 9.00 mmol) was dissolved in 18 mL of a 3:1 v/v mixture of DCE and MeCN under nitrogen. S_2Cl_2 (2.89 mL, 36.0 mmol) was added via syringe into the reaction flask, and the solution was refluxed for 2.5 h. After the allotted reaction time, the dark green solution was cooled to room temperature (rt) and then to 0 °C, and the subsequent red crystals were isolated by filtration, then washed with 3 × 50 mL DCE to give a crude yield of 2.91 g (6.39 mmol, 71%). The product [**1b**][OTf] was dissolved in 100 mL of hot MeCN, the solution hot filtered and concentrated to 50 mL, then cooled to room temperature. The red lustrous crystals were filtered off and washed with DCE, recovery 1.73 g; mp 251−252 °C. IR: 1506 (s), 1268 (s), 1242 (s), 1226 (s), 1172 (m), 1124 (m), 1027 (s), 789 (s), 714 (m), 679 (s), 651 (w), 638 (s), 516 (w), 472 (m) cm^{-1}. Anal. Calcd for $C_{10}H_9F_4N_3O_3S_5$: C, 26.37; H, 1.99; N, 9.22. Found: C, 26.47; H, 2.10; N, 9.14.

Preparation of 8-Fluoro-4-butyl-4*H*-bis([1,2,3]dithiazolo)-[4,5-*b*:5′,4′-*e*]pyridin-2-yl 1b. Decamethylferrocene (0.552 g, 1.69 mmol) was added to a solution of [**1b**] [OTf] (0.700 g, 1.54 mmol) in 13 mL of bubble degassed MeCN. The slurry was stirred on ice for 4 h. After the allotted reaction time, the brown, matte solid was filtered off, and washed with freshly distilled MeCN to give a green microcrystalline solid **1b** (0.389 g, 83%). Crystals suitable for crystallographic work were obtained by vacuum sublimation of the bulk material at 10^{-4} Torr in a three-zone furnace along a temperature gradient of 140 to 60 °C. High quality material for transport property measurements was obtained by recrystallization of 100 mg of crude radical in 10 mL of hot heptane; dec >110 °C. IR: 1502 (w), 1481 (s), 1312 (m), 1249 (m), 1223 (m), 1114 (w), 1100 (s), 821 (m), 769 (m), 734 (w), 685 (m), 652 (m), 478 (w), 462 (w) cm^{-1}. Anal. Calcd for $C_9H_9FN_3S_4$: C, 35.27; H, 2.96; N, 13.71. Found: C, 35.38; H, 3.20; N, 13.73.

Preparation of *N*-pentyl-2,4,6-trifluoro-pyridinium Trifluoromethanesulfonate 5 (R_1 = Pn). A mixture of pentyl triflate (3.82 g, 17.35 mmol) and 2,4,6-trifluoropyridine **4** (2.77 g, 20.82 mmol) was stirred and heated in an oil bath at 60 °C for 16 h. After the allotted reaction time, the product was dried in vacuo, after which the experimental ^{1}H NMR chemical shifts in CD_3CN compared well with literature values of related compounds.[20,45] This material was used in subsequent steps without further purification.

Preparation of *N*-pentyl-2,6-diamino-4-fluoropyridinium Trifluoromethanesulfonate 6 (R_1 = Pn). The product **5** (R_1 = Pn, 7.27 g, ~ 20.0 mmol) was dissolved in 50 mL of MeCN and cooled in an ice bath, over which ammonia gas was passed for 15 min, generating NH_4F as a white precipitate. The NH_4F was filtered off , and the solvent flash evaporated to leave a white crystalline powder, which was recrystallized with DCE/MeCN (10:1) to afford colorless crystals of **6** (R_1 = Pn), yield: 4.05 g (12 mmol, 57%); mp 149−152 °C. IR: 3425 (w), 3352 (m), 3238 (s), 3115 (w), 1682 (m), 1644 (s), 1601 (s), 1455 (m), 1278 (s), 1245 (s), 1172 (s), 1024 (s), 807 (w), 637 (w) cm^{-1}. ^{1}H NMR (δ, CD_3CN): 6.27 (s, 4H, NH_2), 5.96 (d, 2H, J = 9.0 Hz), 3.77 (t, 2H, J = 8.4 Hz), 1.38 (m, 4H), 0.91 (m, 3H). Anal. Calcd for $C_{11}H_{17}F_4N_3O_3S$: C, 38.04; H, 4.93; N, 12.10. Found: C, 38.18; H, 4.98; N, 12.23.

Preparation of 8-Fluoro-4-pentyl-4*H*-bis([1,2,3]dithiazolo)-[4,5-*b*:5′,4′-*e*]pyridin-2-ium Trifluoromethanesulfonate [1c][OTf]. The *N*-pentyl pyridinium triflate salt **6** (1.5 g, 4.31 mmol) was dissolved in 10 mL of a 3:1 v/v mixture of DCE and MeCN under nitrogen. S_2Cl_2 (1.38 mL, 17.19 mmol) was added via syringe into the reaction flask, and the solution was refluxed for 2.5 h. After the allotted reaction time, the dark green solution was cooled to 0 °C, and the subsequent red crystals were isolated by filtration, then washed with 5 × 30 mL of DCE. The product [**1c**][OTf] was redissolved in 100 mL of refluxing MeCN, the solution hot filtered and concentrated to 30 mL, then cooled to room temperature for 1 h and then at 0 °C. The red lustrous crystals were filtered off and washed with DCE, yield 0.938 g (2.00 mmol, 46%); mp 261−262 °C. IR: 1506 (s), 1270 (m), 1246 (s), 1226 (m), 1167 (w), 1030 (m), 789 (m), 714 (w), 678 (w), 637 (m), 471 (m) cm^{-1}. Anal. Calcd for $C_{11}H_{11}F_4N_3O_3S_5$: C, 28.14; H, 2.36; N, 8.95. Found: C, 28.05; H, 2.40; N, 8.91.

Preparation of 8-Fluoro-4-pentyl-4*H*-bis([1,2,3]dithiazolo)-[4,5-*b*:5′,4′-*e*]pyridin-2-yl 1c. Decamethylferrocene (0.255 g, 0.781 mmol) was added to a solution of [**1c**] [OTf] (0.745 g, 1.14 mmol) in 9 mL of bubble degassed MeCN. The slurry was stirred on an ice bath for 2 h. After the allotted reaction time, the brown, matte solid was filtered off, washed with 5 × 10 mL of freshly distilled MeCN, yield 188 mg, 79%. Recrystallization of 150 mg of crude **1c** from 10 mL of hot, degassed (via four freeze−pump−thaw cycles) heptane afforded black/green needles suitable for single crystal X-ray diffraction; dec >120 °C. IR: 1498 (m), 1481 (s), 1365 (m), 1315 (m), 1286 (w), 1236 (s), 1219 (s), 1100 (vs), 821 (m), 772 (m), 756 (m), 733 (w), 684 (m), 651 (m), 460 (m) cm^{-1}. Anal. Calcd for $C_{10}H_{11}FN_3S_4$: C, 37.48; H, 3.46; N, 13.11. Found: C, 37.27; H, 3.69; N, 12.85.

Preparation of *N*-hexyl-2,4,6-trifluoro-pyridinium Trifluoromethanesulfonate 5 (R_1 = Hx). A mixture of hexyl triflate (4.37 g, 18.7 mmol) and 2,4,6-trifluoropyridine **4** (1.65 g, 12.4 mmol) was stirred and heated in an oil bath at 70 °C for 16 h. After the allotted reaction time, the product obtained was dried in vacuo, after which the experimental ^{1}H NMR chemical shifts in CD_3CN compared well with literature values of related compounds.[20,45] The product was used in subsequent steps without further purification.

Preparation of *N*-hexyl-2,6-diamino-4-fluoropyridinium Trifluoromethanesulfonate 6 (R_1 = Hx). The product **5** (R_1 = Hx, ~ 4.6 g, ~ 12.4 mmol) was dissolved in 50 mL of MeCN and cooled in an ice bath, over which ammonia gas was passed for 15 min, generating NH_4F as a white precipitate. The NH_4F was filtered off, and the solvent flash evaporated to leave a white crystalline powder, which was recrystallized with 20 mL of DCE/MeCN (10:1) to afford colorless crystals of **6** (R_1 = Hx), yield: 2.07 g (5.97 mmol, 48% over two steps); mp 130−131 °C. IR: 3424 (m), 3355 (m), 3239 (s), 3116 (w), 1684 (m), 1645 (s), 1601 (s), 1515 (m), 1345 (w), 1276 (vs), 1245 (vs), 1220 (s), 1171 (s), 1079 (w), 1024 (vs), 807 (m), 762 (w), 639 (s), 597 (m), 574 (w), 532 (w), 515 (m) cm^{-1}. ^{1}H NMR (δ, CD_3CN): 6.23 (s, 2H), 5.94 (d, 1H, J = 9.3 Hz), 3.76 (m, 2H), 1.65 (m, 2H), 1.41 (m, 2H), 1.33 (m, 2H), 0.89 (t, 3H, J = 6.3 Hz). Anal. Calcd for $C_{12}H_{19}F_4N_3O_3S$: C, 39.89; H, 5.30; N, 11.63. Found: C, 39.77; H, 5.48; N, 11.86.

Preparation of 8-Fluoro-4-hexyl-4*H*-bis([1,2,3]dithiazolo)-[4,5-*b*:5′,4′-*e*]pyridin-2-ium Trifluoromethanesulfonate [1d][OTf]. The *N*-hexyl pyridinium triflate salt **6** (1.02 g, 2.82 mmol) was dissolved in 7 mL of a 5:2 mixture of DCE and MeCN under nitrogen. S_2Cl_2 (0.90 mL, 11.3 mmol) was added via syringe into the reaction flask, and the solution was refluxed for 2 h. After the allotted reaction time, the dark green solution was cooled to room temperature and then to 0 °C, and the subsequent red crystals were

dx.doi.org/10.1021/ic302658c | Inorg. Chem. 2013, 52, 2188−2198

isolated by filtration, then washed with 3 × 10 mL of DCE. The product [**1d**][OTf] was redissolved in 100 mL of hot MeCN, the solution hot filtered and concentrated to 25 mL, then cooled to room temperature for 1 h and then at 0 °C for 1 h. The red lustrous crystals were filtered off and washed with DCE, yield 0.49 g (2.00 mmol, 36%); mp 270−272 °C. IR: 1506 (s), 1270 (s), 1246 (s), 1226 (s), 1167 (s), 1119 (m), 1030 (s), 910 (w), 868 (w), 789 (s), 769 (w), 758 (w), 714 (m), 678 (m), 679 (m), 650 (m), 638 (s), 573 (w), 516 (m), 473 (s) cm^{-1}. Anal. Calcd for $C_{12}H_{13}F_4N_3O_3S_5$: C, 29.80; H, 2.71; N, 8.69. Found: C, 30.07; H, 2.50; N, 8.44.

Preparation of 8-Fluoro-4-hexyl-4*H*-bis([1,2,3]dithiazolo)-[4,5-*b*:5′,4′-*e*]pyridin-2-yl 1d. Decamethylferrocene (0.454 g, 1.39 mmol) was added to a solution of [**1d**] [OTf] (0.641 g, 1.32 mmol) in 15 mL of bubble degassed MeCN. The slurry was stirred at 0 °C for 3 h. After the allotted reaction time, the brown, matte solid was filtered off, washed with 5 × 10 mL of freshly distilled MeCN, yield 388 mg (88%). Recrystallization of 100 mg of crude **1d** from 10 mL of hot, degassed (via four freeze−pump−thaw cycles) heptane afforded black/green needles suitable for single crystal X-ray diffraction; dec >150 °C IR: 1500 (m), 1481 (s), 1374 (m), 1314 (m), 1300 (w), 1267 (w), 1234 (s), 1212 (m), 1099 (s), 822 (m), 769 (m), 727 (w), 685 (m), 652 (m), 477 (w), 461 (m), 422 (w) cm^{-1}. Anal. Calcd for $C_{12}H_{19}F_4N_3O_3S$: C, 39.50; H, 3.92; N, 12.56. Found: C, 39.36; H, 3.93; N, 12.36.

Preparation of 8-Chloro-4-pentyl-4*H*-bis([1,2,3]dithiazolo)-[4,5-*b*:5′,4′-*e*]pyridin-2-ium Trifluoromethanesulfonate [1][OTf] (R_1 = Pn, R_2 = Cl). A sample of zwitterionic ClBP[12b] (0.544 g, 1.55 mmol) and PnOTf (0.444 g, 2.02 mmol) were dissolved in 10 mL of freshly distilled DCE and stirred at room temperature for 24 h. After the allotted reaction time, the crystals were filtered off, washed twice with DCM. The product was redissolved in 50 mL of refluxing MeCN, the solution hot filtered, and concentrated to 10 mL, then cooled to room temperature and then to 0 °C, yield 0.555 g (1.14 mmol, 74%). IR: 1515 (w), 1488 (s), 1450 (s), 1362 (s), 1267 (s), 1248 (s), 1223 (m), 1165 (m), 1028 (s), 767 (m), 673 (w), 637 (m), 482 (m) cm^{-1}. Anal. Calc'd for $C_{10}H_9ClF_3N_3O_3S_5$: C, 25.45; H, 1.92; N, 8.90. Found: C, 25.44; H, 1.93; N, 8.77.

Preparation of 8-Chloro-4-butyl-4*H*-bis([1,2,3]dithiazolo)-[4,5-*b*:5′,4′-*e*]pyridin-2-ium Trifluoromethanesulfonate [1][OTf] (R_1 = Bu, R_2 = Cl). A sample of zwitterionic ClBP[12b] (0.545 g, 1.55 mmol) and BuOTf (0.416 g, 2.02 mmol) were dissolved in 30 mL of freshly distilled DCE and stirred at room temperature for 48 h. After the allotted reaction time, the crystals were filtered, washed twice with DCM. The product was redissolved in 75 mL of refluxing MeCN, the solution hot filtered, and concentrated to 20 mL, then cooled to room temperature and then to 0 °C, yield 0.408 g (0.733 mmol, 47%). Anal. Calc'd for $C_{11}H_{11}ClF_3N_3O_3S_5$: C, 27.18; H, 2.28; N, 8.65. Found: C, 27.06; H, 2.32; N, 8.59.

EPR Spectroscopy. The X-band EPR spectra of **1a−d** were recorded at ambient temperature on a Bruker EMX-200 spectrometer using a sample of radical dissolved in degassed DCM. Hyperfine coupling constants were obtained by spectral simulation using Simfonia[30] and WinSim.

Crystallography. Crystals were glued to glass fibers with epoxy. X-ray data for **1a** and **1b** were collected using ω scans with a Bruker APEX I CCD detector on a D8 3-circle goniometer and Mo Kα (λ = 0.71073 Å) radiation. The data were scanned using Bruker's SMART program and integrated using Bruker's SAINT software.[46] X-ray data for **1c** were collected using ω and φ scans with a Bruker SMART 6000 CCD detector on a 3-circle goniometer and Cu Kα (λ = 1.5418 Å) radiation. The data were scanned using Bruker's SMART program, integrated using Bruker's SAINT software, and corrected for absorption via using SADABS,[47] all as part of the Apex II software suite (Bruker 2010).[48] X-ray data for **1d** were collected using ω and φ scans with a Bruker APEX II CCD detector on a 3-circle goniometer and Mo Kα (λ = 0.71073 Å) radiation. The data were scanned using Bruker's SMART program, integrated using Bruker's SAINT software and corrected for absorption via face-indexing and redundant data (SADABS) all as part of the Apex II software suite (Bruker 2010). All of the structures were solved by direct methods using SHELXS-97[49] and refined by least-squares methods on F^2 using SHELXL-97[50] incorporated in the SHELXTL[51] suite of programs.

Magnetic Susceptibility Measurements. DC magnetic susceptibility measurements on **1a−d** were performed over the temperature range 2−300 K on a Quantum Design MPMS SQUID magnetometer. Diamagnetic corrections were made using Pascal's constants.[52]

Exchange Energy Calculations. All calculations were performed using the UB3LYP functional and the split-valence double-ζ basis set 6-31G(d,p), as contained in the Gaussian 09W suite of programs.[53] Exchange energies of interacting pairs of radicals (Figure 11) were computed from single point energies of the triplet and broken symmetry singlet states and their respective $\langle S^2 \rangle$ expectation values. Tight convergence criteria were employed, and atomic coordinates were taken from crystallographic data.

■ ASSOCIATED CONTENT

Ⓢ Supporting Information

Details of single crystal X-ray crystallographic data collection and structure refinement, tables of atomic coordinates, bond distances and angles, anisotropic thermal parameters, and hydrogen atom positions in CIF format are available. Details of DFT magnetic exchange energy calculation results and of the magnetic fits are provided. This material is available free of charge via the Internet at http://pubs.acs.org.

■ AUTHOR INFORMATION

Corresponding Author

*E-mail: oakley@uwaterloo.ca.

Notes

The authors declare no competing financial interest.

■ ACKNOWLEDGMENTS

We thank the Natural Sciences and Engineering Research Council of Canada (NSERCC) for financial support, for a Vanier Graduate Scholarship to K.L. and a postgraduate scholarship to S.M.W.

■ REFERENCES

(1) (a) Haddon, R. C. *Nature* **1975**, *256*, 394. (b) Haddon, R. C. *Aust. J. Chem.* **1975**, *28*, 2333. (c) Haddon, R. C. *Aust. J. Chem.* **1975**, *28*, 2343.

(2) (a) Goto, K.; Kubo, T.; Yamamoto, K.; Nakasuji, K.; Sato, K.; Shiomi, D.; Takui, T.; Kubota, M.; Kobayashi, T.; Yakusi, K.; Ouyang, J. *J. Am. Chem. Soc.* **1999**, *121*, 1619. (b) Koutentis, P. A.; Chen, Y.; Cao, Y.; Best, T. P.; Itkis, M. E.; Beer, L.; Oakley, R. T.; Brock, C. P.; Haddon, R. C. *J. Am. Chem. Soc.* **2001**, *123*, 3864. (c) Takano, Y.; Taniguchi, T.; Isobe, H.; Kubo, T.; Morita, Y.; Yamamoto, K.; Nakasuji, K.; Takui, T.; Yamaguchi, K. *J. Am. Chem. Soc.* **2002**, *124*, 11122. (d) Beer, L.; Mandal, S. K.; Reed, R. W.; Oakley, R. T.; Tham, F. S.; Donnadieu, B.; Haddon, R. C. *Cryst. Growth Des.* **2007**, *7*, 101. (e) Beer, L.; Reed, R. W.; Robertson, C. M.; Oakley, R. T.; Tham, F. S.; Haddon, R. C. *Org. Lett.* **2008**, *10*, 3121. (f) Morita, Y.; Nishida, S. In *Stable Radicals: Fundamentals and Applied Aspects of Odd-Electron Compounds*; Hicks, R. G., Ed.; John Wiley & Sons, Ltd.: Wiltshire, U.K., 2010; pp 81−145. (g) Morita, Y.; Suzuki, S.; Sato, K.; Takui, T. *Nat. Chem.* **2011**, *3*, 197.

(3) (a) Chi, X.; Itkis, M. E.; Patrick, B. O.; Barclay, T. M.; Reed, R. W.; Oakley, R. T.; Cordes, A. W.; Haddon, R. C. *J. Am. Chem. Soc.* **1999**, *121*, 10395. (b) Mandal, S. K.; Samanta, S.; Itkis, M. E.; Jensen, D. W.; Reed, R. W.; Oakley, R. T.; Tham, F. S.; Donnadieu, B.; Haddon, R. C. *J. Am. Chem. Soc.* **2006**, *128*, 1982. (c) Haddon, R. C.; Sarkar, A.; Pal, S. K.; Chi, X.; Itkis, M. E.; Tham, F. S. *J. Am. Chem. Soc.* **2008**, *130*, 13683. (d) Pal, S. K.; Itkis, M. E.; Tham, F. S.; Reed, R. W.; Oakley, R. T.; Haddon, R. C. *J. Am. Chem. Soc.* **2008**, *130*, 3942. (e) Bag, P.; Itkis, M. E.; Pal, S. K.; Donnadieu, B.; Tham, F. S.; Park, H.; Schlueter, J. A.; Siegrist, T.; Haddon, R. C. *J. Am. Chem. Soc.* **2010**,

132, 2684. (f) Kubo, T.; Katada, Y.; Shimizu, A.; Hirao, Y.; Sato, K.; Takui, T.; Uruichi, M.; Yakushi, K.; Haddon, R. C. *J. Am. Chem. Soc.* **2011**, *133*, 14240.

(4) (a) Lahti, P. *Adv. Phys. Org. Chem.* **2011**, *45*, 93. (b) Karoui, H.; Le Moigne, F.; Ouari, O.; Tordo, P. In *Stable Radicals: Fundamentals and Applied Aspects of Odd-Electron Compounds*; Hicks, R. G., Ed.; John Wiley & Sons, Ltd.: Wiltshire, U.K., 2010; pp 173−229.

(5) (a) Ratera, I.; Veciana, J. *Chem. Soc. Rev.* **2012**, *41*, 303. (b) Hicks, R. G. In *Stable Radicals: Fundamentals and Applied Aspects of Odd-Electron Compounds*; Hicks, R. G., Ed.; John Wiley & Sons, Ltd.: Wiltshire, U.K., 2010; pp 248−280. (c) Saito, G.; Yoshida, Y. *Bull. Chem. Soc. Jpn.* **2007**, *80*, 1. (d) Hicks, R. G. *Org. Biomol. Chem.* **2007**, *5*, 1321.

(6) (a) Blatter, H. M.; Lukaszewski, H. *Tetrahedron Lett.* **1968**, *9*, 2701. (b) Constantinides, C. P.; Koutentis, P. A.; Krassos, H.; Rawson, J. M.; Tasiopoulos, A. J. *J. Org. Chem.* **2011**, *76*, 2798. (c) Constantinides, C. P.; Koutentis, P. A.; Rawson, J. M. *Chem.—Eur. J.* **2012**, *18*, 7109. (d) Yan, B.; Cramen, J.; McDonald, R.; Frank, N. L. *Chem. Commun.* **2011**, *47*, 3201. (e) Berezin, A. A.; Constantinides, C. P.; Drouza, C.; Manoli, M.; Koutentis, P. A. *Org. Lett.* **2012**, *14*, 5586.

(7) (a) Tamura, M.; Nakazawa, Y.; Shiomi, D.; Nozawa, K.; Hosokoshi, Y.; Ishikawa, M.; Takahashi, M.; Kinoshita, M. *Chem. Phys. Lett.* **1991**, *186*, 401. (b) Chiarelli, R.; Novak, M. A.; Rassat, A.; Tholence, J. L. *Nature* **1993**, *363*, 147.

(8) Mito, M.; Nakano, H.; Kawae, T.; Hitaka, M.; Takagi, S.; Deguchi, H.; Suzuki, K.; Mukai, K.; Takeda, K. J. *Phys. Soc. Jpn.* **1997**, *66*, 2147.

(9) (a) Cordes, A. W.; Haddon, R. C.; Oakley, R. T. *Adv. Mater.* **1994**, *6*, 798. (b) Oakley, R. T. *Can. J. Chem.* **1993**, *71*, 1775. (c) Rawson, J. M.; Alberola, A.; Whalley, A. *J. Mater. Chem.* **2006**, *16*, 2560. (d) Haynes, D. A. *CrystEngComm* **2011**, *13*, 4793. (e) Rakitin, O. A. *Russ. Chem. Rev.* **2011**, *80*, 647. (f) Hicks, R. G. In *Stable Radicals: Fundamentals and Applied Aspects of Odd-Electron Compounds*; Hicks, R. G., Ed.; John Wiley & Sons, Ltd.: Wiltshire, U.K., 2010; pp 317−380.

(10) Beneberu, H. Z.; Tian, Y.-H.; Kertesz, M. *Phys. Chem. Chem. Phys.* **2012**, *14*, 10713.

(11) (a) Banister, A. J.; Bricklebank, N.; Lavender, I.; Rawson, J. M.; Gregory, C. I.; Tanner, B. K.; Clegg, W.; Elsegood, M. R. J.; Palacio, F. *Angew. Chem., Int. Ed. Engl.* **1996**, *35*, 2533. (b) Alberola, A.; Less, R. J.; Pask, C. M.; Rawson, J. M.; Palacio, F.; Oliete, P.; Paulsen, C.; Yamaguchi, A.; Farley, R. D.; Murphy, D. M. *Angew. Chem., Int. Ed.* **2003**, *42*, 4782. (c) Barclay, T. M.; Cordes, A. W.; George, N. A.; Haddon, R. C.; Itkis, M. E.; Mashuta, M. S.; Oakley, R. T.; Patenaude, G. W.; Reed, R. W.; Richardson, J. F.; Zhang, H. *J. Am. Chem. Soc.* **1998**, *120*, 352. (d) Fujita, W.; Awaga, K. *Science* **1999**, *281*, 261. (e) McManus, G. D.; Rawson, J. M.; Feeder, N.; van Duijn, J.; McInnes, E. J. L.; Novoa, J. J.; Burriel, R.; Palacio, F.; Oliete, P. *J. Mater. Chem.* **2001**, *11*, 1992. (f) Brusso, J. L.; Clements, O. P.; Haddon, R. C.; Itkis, M. E.; Leitch, A. A.; Oakley, R. T.; Reed, R. W.; Richardson, J. F. *J. Am. Chem. Soc.* **2004**, *126*, 14692.

(12) (a) Cordes, A. W.; Haddon, R. C.; Oakley, R. T. *Phosphorus, Sulfur, Silicon Relat. Elem.* **2004**, *179*, 673. (b) Beer, L.; Brusso, J. L.; Cordes, A. W.; Haddon, R. C.; Itkis, M. E.; Kirschbaum, K.; MacGregor, D. S.; Oakley, R. T.; Pinkerton, A. A.; Reed, R. W. *J. Am. Chem. Soc.* **2002**, *124*, 9498. (c) Beer, L.; Britten, J. F.; Brusso, J. L.; Cordes, A. W.; Haddon, R. C.; Itkis, M. E.; MacGregor, D. S.; Oakley, R. T.; Reed, R. W.; Robertson, C. M. *J. Am. Chem. Soc.* **2003**, *125*, 14394. (d) Beer, L.; Britten, J. F.; Clements, O. P.; Haddon, R. C.; Itkis, M. E.; Matkovich, K. M.; Oakley, R. T.; Reed, R. W. *Chem. Mater.* **2004**, *16*, 1564.

(13) (a) Yu, X.; Mailman, A.; Dube, P. A.; Assoud, A.; Oakley, R. T. *Chem. Commun.* **2011**, *47*, 2011, 4655. (b) Yu, X.; Mailman, A.; Lekin, K.; Assoud, A.; Robertson, C. M.; Noll, B. C.; Campana, C. F.; Howard, J. A. K.; Dube, P. A.; Oakley, R. T. *J. Am. Chem. Soc.* **2012**, *134*, 2264. (c) Yu, X.; Mailman, A.; Lekin, K.; Assoud, A.; Dube, P. A.; Oakley, R. T. *Cryst. Growth Des.* **2012**, *12*, 2485. (d) Mailman, A.; Winter, S. M.; Yu, X.; Robertson, C. M.; Yong, W.; Tse, J. S.; Secco, R. A.; Liu, Z.; Dube, P. A.; Howard, J. A. K.; Oakley, R. T. *J. Am. Chem. Soc.* **2012**, *134*, 9886.

(14) Winter, S. M.; Cvrkalj, K.; Robertson, C. M.; Probert, M. R.; Dube, P. A.; Howard, J. A. K.; Oakley, R. T. *Chem. Commun.* **2009**, 7306.

(15) (a) Winter, S. M.; Datta, S.; Hill, S.; Oakley, R. T. *J. Am. Chem. Soc.* **2012**, *133*, 8126. (b) Winter, S. M.; Oakley, R. T.; Kovalev, A. E.; Hill, S. *Phys. Rev. B* **2012**, *85*, 094430. (c) Pivtsov, A. V.; Kulik, L. V.; Makarov, A. Y.; Blockhuys, F. *Phys. Chem. Chem. Phys.* **2011**, *13*, 3873.

(16) Leitch, A. A.; Brusso, J. L.; Cvrkalj, K.; Reed, R. W.; Robertson, C. M.; Dube, P. A.; Oakley, R. T. *Chem. Commun.* **2007**, 3368.

(17) (a) Robertson, C. M.; Leitch, A. A.; Cvrkalj, K.; Reed, R. W.; Myles, D. J. T.; Dube, P. A.; Dube, Oakley, R. T. *J. Am. Chem. Soc.* **2008**, *130*, 8414. (b) Robertson, C. M.; Leitch, A. A.; Cvrkalj, K.; Myles, D. J. T.; Reed, R. W.; Dube, P. A.; Oakley, R. T. *J. Am. Chem. Soc.* **2008**, *130*, 14791. (c) Leitch, A. A.; Lekin, K.; Winter, S. M.; Downie, L. E.; Tsuruda, H.; Tse, J. S.; Mito, M.; Desgreniers, S.; Dube, P. A.; Zhang, S.; Liu, Q.; Jin, C.; Ohishi, Y.; Oakley, R. T. *J. Am. Chem. Soc.* **2011**, *133*, 6051.

(18) (a) Brusso, J. L.; Cvrkalj, K.; Leitch, A. A.; Oakley, R. T.; Reed, R. W.; Robertson, C. M. *J. Am. Chem. Soc.* **2006**, *128*, 15080. (b) Leitch, A. A.; Yu, X.; Winter, S. M.; Secco, R. A.; Dube, P. A.; Oakley, R. T. *J. Am. Chem. Soc.* **2009**, *131*, 7112. (c) Brusso, J. L.; Derakhshan, S.; Itkis, M. E.; Kleinke, H.; Haddon, R. C.; Oakley, R. T.; Reed, R. W.; Richardson, J. F.; Robertson, C. M.; Thompson, L. K. *Inorg. Chem.* **2006**, *45*, 10958.

(19) (a) Desiraju, G. R. *Angew. Chem., Int. Ed. Engl.* **1995**, *34*, 2311. (b) Desiraju, D. G. *Acc. Chem. Res.* **2002**, *35*, 565. (c) Thakur, T. S.; Kirchner, M. T.; Bläser, D.; Boese, R.; Desiraju, D. R. *CrystEngComm* **2010**, *12*, 2079.

(20) Lekin, K.; Winter, S. M.; Downie, L. E.; Bao, X.; Tse, J. S.; Desgreniers, S.; Secco, R. A.; Dube, P. A.; Oakley, R. T. *J. Am. Chem. Soc.* **2010**, *132*, 16212.

(21) Rovira, C. *Chem.—Eur. J.* **2000**, *6*, 1723.

(22) (a) Uehara, M.; Nagata, T.; Akimitsu, J.; Takahashi, H.; Mori, N.; Kinoshita, K. *J. Phys. Soc. Jpn.* **1996**, *65*, 2764. (b) Nakanishi, T.; Motoyama, N.; Mitamura, H.; Takeshita, N.; Takahashi, H.; Eisaki, H.; Uchida, S.; Mori, N. *Phys. Rev. B* **2005**, *72*, 054520. (c) Vuletic, T.; Korin-Hamzic, B.; Ivek, T.; Tomic, S.; Gorshunov, B.; Dressel, M.; Akimitsu. *J. Phys. Rep.* **2006**, *428*, 169. (d) Carter, S. A.; Batlogg, B.; Cava, R. J.; Krajewski, J. J.; Peck, W. F., Jr.; Rice, T. M. *Phys. Rev. Lett.* **1996**, *77*, 1378. (e) Azuma, M.; Hiroi, Z.; Takano, M.; Ishida, K.; Kitaoka, Y. *Phys. Rev. Lett.* **1994**, *73*, 3463. (f) Gozar, A.; Blumberg, G.; Dennis, B. S.; Shastry, N.; Motoyama, N.; Eisaki, H.; Uchida, S. *Phys. Rev. Lett.* **2001**, *87*, 197202. (g) Moshchalkov, V. V.; Trappeniers, L.; Vanacken, J. *Europhys. Lett.* **1999**, *46*, 75.

(23) (a) White, J. L.; Lee, C.; Günaydin-Şen, Ö; Tung, L. C.; Christen, H. M.; Wang, Y. J.; Turnbull, M. M.; Landee, C. P.; McDonald, R. D.; Crooker, S. A.; Singleton, J.; Whangbo, M.-H.; Musfeldt, J. L. *Phys. Rev. B* **2010**, *81*, 052407. (b) Matsumoto, T.; Miyazaki, Y.; Albrecht, A. S.; Landee, C. P.; Turnbull, M. M.; Sorai, M. *J. Phys. Chem. B* **2000**, *104*, 9993. (c) Woodward, F. M.; Albrecht, A. S.; Wynn, C. M.; Landee, C. P.; Turnbull, M. M. *Phys. Rev. B* **2002**, *65*, 144412. (d) Awwadi, F.; Willett, R. D.; Twamley, B.; Schneider, R.; Landee, C. P. *Inorg. Chem.* **2008**, *47*, 9327. (e) Willett, R. D.; Galeriu, C.; Landee, C. P.; Turnbull, M. M.; Twamley, B. *Inorg. Chem.* **2004**, *43*, 3804. (f) Shapiro, A.; Landee, C. P.; Turnbull, M. M.; Jornet, J.; Deumal, M.; Novoa, J. J.; Robb, M. A.; Lewis, W. *J. Am. Chem. Soc.* **2007**, *129*, 952.

(24) (a) Yoshida, Y.; Tateiwa, N.; Mito, M.; Kawae, T.; Takeda, K.; Hosokoshi, Y.; Inoue, K. *Phys. Rev. Lett.* **2005**, *94*, 037203. (b) Kikuchi, M.; Okamoto, K.; Okunishi, K.; Sakai, T. *Prog. Theor. Phys. Suppl.* **2005**, *159*, 251. (c) Sakai, T.; Okamoto, K.; Okunishi, K.; Kindo, K.; Narumi, Y.; Hosokoshi, Y.; Katoh, K.; Inoue, K.; Goto, T. *Phys. B (Amsterdam, Neth.)* **2004**, *346*, 34. (d) Tamura, M.; Hosokoshi, Y.; Shiomi, D.; Kinoshita, M.; Nakasawa, Y.; Ishikawa, M.; Sawa, H.; Kitazawa, T.; Eguchi, A.; Nishio, Y.; Kajita, K. *J. Phys. Soc. Jpn.* **2003**, *72*, 1735.

(25) (a) Ribas, X.; Mas-Torrent, M.; Pérez-Benítez, A.; Dias, J. S.; Alves, H.; Lopes, E. B.; Henriques, R. T.; Molins, E.; Santos, I. C.; Wurst, K.; Foury-Leylekian, F.; Almeida, M.; Veciana, J.; Rovira, C. *Adv. Funct. Mater.* **2005**, *15*, 1023. (b) Rovira, C. In *Strucure and Bonding (Berlin)*; Veciana, J., Ed.; Springer-Verlag: Berlin, Germany, 2001; pp 163−188.
(26) (a) Schmidt, K. P.; Uhrig, G. S. *Mod. Phys. Lett. B* **2005**, *19*, 1179. (b) Dagotto, E.; Rice, T. M. *Science* **1996**, *271*, 618.
(27) (a) Dagotto, E.; Riera, J.; Scalapino, D. J. *Phys. Rev. B* **1992**, *45*, 5744. (b) Dagotto, E. *Rep. Prog. Phys.* **1999**, *62*, 1525.
(28) Shaterian, H. R.; Doostmohammadi, R.; Ghashang, M. *Chin. J. Chem.* **2008**, *26*, 1709.
(29) X-ray quality crystals of **1b** can be grown via vacuum sublimation and recrystallization from heptane; however, the X-ray data was obtained for crystals from sublimation, while the transport property measurements were performed on recrystallized material (easier to obtain in bulk quantities). Material from both procedures was deemed phase pure via FTIR, and the phases were identical to each other.
(30) *WinEPR Simfonia*, version 1.25; Bruker Instruments, Inc.: Billerica, MA, 1996.
(31) (a) Bondi, A. *J. Phys. Chem.* **1964**, *68*, 441. (b) Dance, I. *New J. Chem.* **2003**, *27*, 22.
(32) (a) Bonner, J. C.; Fisher, M. E. *Phys. Rev.* **1964**, *135*, A640. (b) Estes, W. E.; Gavel, D. P.; Hatfield, W. E.; Hodgson, D. J. *Inorg. Chem.* **1978**, *17*, 1415.
(33) Details of the Bonner−Fisher fit for the magnetic data of **1a** are provided in the Supporting Information.
(34) Slippage coordinates for **1a** are (*dx* = 0 Å, *dy* = 2.49 Å) and for *α*-**1** (R_1 = Et, R_2 = F) are (*dx* = 0 Å, *dy* = 2.20 Å).
(35) Bleaney, B.; Bowers, K. D. *Proc. R. Soc. London, A* **1952**, 214.
(36) Gu, Q.; Yu, D.-K.; Shen, J.-L. *Phys. Rev. B* **1999**, *60*, 3009.
(37) Landee, C. P.; Turnbull, M. M.; Galeriu, C.; Giantsidis, J.; Woodward, F. M. *Phys. Rev. B* **2001**, *63*, 100402.
(38) (a) Johnston, D. C.; Troyer, M.; Miyahara, S.; Lidsky, D.; Ueda, K.; Azuma, M.; Hiroi, Z.; Takano, M.; Isobe, M.; Ueda, Y.; Korotin, M. A.; Anisimov, V. I.; Mahajan, A. V.; Miller, L. L. *arXiv:cond-mat/0001147*.
(39) (a) Noodleman, L. *J. Chem. Phys.* **1981**, *74*, 5737. (b) Noodleman, L.; Davidson, E. R. *Chem. Phys.* **1986**, *109*, 131. (c) Nagao, H.; Nishino, M.; Shigeta, Y.; Soda, T.; Kitagawa, Y.; Onishi, T.; Yoshioka, Y.; Yamaguchi, K. *Coord. Chem. Rev.* **2000**, *198*, 265. (d) Noodleman, L.; Norman, J. G. *J. Chem. Phys.* **1979**, *70*, 4903.
(40) (a) Deumal, M.; Robb, M. A.; Novoa, J. J. *Prog. Theor. Chem. Phys.* **2007**, *16*, 271. (b) Li, L.; Turnbull, M. M.; Landee, C. P.; Jornet, J.; Deumal, M.; Novoa, J. J.; Wikaira, J. L. *Inorg. Chem.* **2007**, *46*, 11254.
(41) QMC simulations employed the *looper* code implemented in ALPS project distribution 2.0; see (a) Todo, S.; Kato, K. *Phys. Rev. Lett.* **2001**, *87*, 047203. (b) Bauer, B.; Carr, L. D.; Evertz, H. G.; Feiguin, A.; Freire, J.; Fuchs, S.; Gamper, L.; Gukelberger, J.; Gull, E.; Guertler, S.; Hehn, A.; Igarashi, R.; Isakov, S. V.; Koop, D.; Me, P. N.; Mates, P.; Matsuo, H.; Parcollet, O.; Pawłowski, G.; Picon, J. D.; Pollet, L.; Santos, E.; Scarola, V. W.; Schollwöck, U.; Silca, C.; Surer, B.; Todo, S.; Trebst, S.; Troyer, M.; Wall, M. L.; Werner, P.; Wessel, S.; (ALPS Collaboration). *J. Stat. Mech.* **2011**, P05001.
(42) Jornet-Somoza, J.; Codina-Castillo, N.; Deumal, M.; Mota, F.; Novoa, J. J.; Butcher, R. T.; Turnbull, M. M.; Keith, B.; Landee, C. P.; Wikaira, J. L. *Inorg. Chem.* **2012**, *51*, 6315.
(43) Lekin, K.; Leitch, A. A.; Tse, J. S.; Bao, X.; Secco, R. A.; Desgreniers, S.; Ohishi, Y.; Oakley, R. T. *Cryst. Growth Des.* **2012**, *12*, 4676.
(44) (a) Desiraju, D. G. *Acc. Chem. Res.* **2002**, *35*, 565. (b) Thakur, T. S.; Kirchner, M. T.; Bläser, D.; Boese, R.; Desiraju, D. R. *CrystEngComm* **2010**, *12*, 2079. (c) Weiss, H.-C.; Boese, R.; Smith, H. L.; Haley, M. M. *Chem. Commun.* **1997**, 2403. (d) Thalladi, V. R.; Weiss, H. C.; Bläser, D.; Boese, R.; Nangia, A.; Desiraju, D. R. *J. Am. Chem. Soc.* **1998**, *120*, 8702. (e) Mele, A.; Vergani, B.; Viani, F.; Meille, S. V.; Farina, A.; Bravo, F. *Eur. J. Org. Chem.* **1999**, 187. (f) Haufe, G.; Rosen, T. C.; Meyer, O. G. J.; Fröhlich, R.; Rissanen, K. *J. Fluorine Chem.* **2002**, *114*, 189. (g) Hyla-Kryspin, E.; Haufe, G.; Grimme, S. *Chem.—Eur. J.* **2004**, *10*, 3411.
(45) Leitch, A. A.; Yu, X.; Robertson, C. M.; Secco, R. A.; Tse, J. S.; Oakley, R. T. *Inorg. Chem.* **2009**, *48*, 9874.
(46) *SAINT*, version 6.22; Bruker Advanced X-ray Solutions, Inc.: Madison, WI, 2001.
(47) Sheldrick, G. M. *SADABS (Version 2008/2), Siemens Area Detector Absorption Correction*; Universitat Göttingen: Göttingen, Germany, 2008.
(48) *Bruker (2010) Apex (Version 2010−1) and SAINT (Version 7.68a)*; Bruker Advanced X-ray Solutions, Inc.: Madison, WI, 2010.
(49) *SHELXS-90*; Sheldrick, G. M. *Acta Crystallogr. A* **1990**, *46*, 467.
(50) Sheldrick, G. M. *SHELXL-97, Program for the Refinement of Crystal Structures*; University of Göttingen: Göttingen, Germany, 1997.
(51) *SHELXTL, Program Library for Structure Solution and Molecular Graphics*, version 6.12; Bruker Advanced X-ray Solutions, Inc.: Madison, WI, 2001.
(52) Carlin, R. L. *Magnetochemistry*; Springer-Verlag: New York, 1986.
(53) Frisch, M. J.; Trucks, G. W.; Schlegel, H. B.; Scuseria, G. E.; Robb, M. A.; Cheeseman, J. R.; Scalmani, G.; Barone, V.; Mennucci, B.; Petersson, G. A.; Nakatsuji, H.; Caricato, M.; Li, X.; Hratchian, H. P.; Izmaylov, A. F.; Bloino, J.; Zheng, G.; Sonnenberg, J. L.; Hada, M.; Ehara, M.; Toyota, K.; Fukuda, R.; Hasegawa, J.; Ishida, M.; Nakajima, T.; Honda, Y.; Kitao, O.; Nakai, H.; Vreven, T.; Montgomery, Jr., J. A.; Peralta, J. E.; Ogliaro, F.; Bearpark, M.; Heyd, J. J.; Brothers, E.; Kudin, K. N.; Staroverov, V. N.; Kobayashi, R.; Normand, J.; Raghavachari, K.; Rendell, A.; Burant, J. C.; Iyengar, S. S.; Tomasi, J.; Cossi, M.; Rega, N.; Millam, N. J.; Klene, M.; Knox, J. E.; Cross, J. B.; Bakken, V.; Adamo, C.; Jaramillo, J.; Gomperts, R.; Stratmann, R. E.; Yazyev, O.; Austin, A. J.; Cammi, R.; Pomelli, C.; Ochterski, J. W.; Martin, R. W.; Morokuma, K.; Zakrzewski, V. G.; Voth, G., A.; Salvador, P.; Dannenberg, J. J.; Dapprich, S.; Daniels, A. D.; Farkas, O.; Foresman, J. B.; Ortiz, J. V.; Cioslowski, J.; Fox, D. J. *Gaussian 09*, revision A.02; Gaussian, Inc.: Wallingford, CT, 2009.